Rab1 Guanine Nucleotide Exchange Factor SidM Is a Major Phosphatidylinositol 4-Phosphate-binding Effector Protein of *Legionella pneumophila*[*][S]

Eva Brombacher[‡], Simon Urwyler[‡], Curdin Ragaz[‡], Stefan S. Weber[‡], Keiichiro Kami[§], Michael Overduin[§1], and Hubert Hilbi[‡2]

From the [‡]Institute of Microbiology, ETH Zürich, Wolfgang-Pauli-Strasse 10, 8093 Zürich, Switzerland and the [§]Cancer Research UK Institute for Cancer Studies, University of Birmingham, Birmingham B15 2TT, United Kingdom

The causative agent of Legionnaires disease, *Legionella pneumophila,* forms a replicative vacuole in phagocytes by means of the intracellular multiplication/defective organelle trafficking (Icm/Dot) type IV secretion system and translocated effector proteins, some of which subvert host GTP and phosphoinositide (PI) metabolism. The Icm/Dot substrate SidC anchors to the membrane of *Legionella*-containing vacuoles (LCVs) by specifically binding to phosphatidylinositol 4-phosphate (PtdIns(4)P). Using a nonbiased screen for novel *L. pneumophila* PI-binding proteins, we identified the Rab1 guanine nucleotide exchange factor (GEF) SidM/DrrA as the predominant PtdIns(4)P-binding protein. Purified SidM specifically and directly bound to PtdIns(4)P, whereas the SidM-interacting Icm/Dot substrate LidA preferentially bound PtdIns(3)P but also PtdIns(4)P, and the *L. pneumophila* Arf1 GEF RalF did not bind to any PIs. The PtdIns(4)P-binding domain of SidM was mapped to the 12-kDa C-terminal sequence, termed "P4M" (PtdIns4P binding of SidM/DrrA). The isolated P4M domain is largely helical and displayed higher PtdIns(4)P binding activity in the context of the α-helical, monomeric full-length protein. SidM constructs containing P4M were translocated by Icm/Dot-proficient *L. pneumophila* and localized to the LCV membrane, indicating that SidM anchors to PtdIns(4)P on LCVs via its P4M domain. An *L. pneumophila* Δ*sidM* mutant strain displayed significantly higher amounts of SidC on LCVs, suggesting that SidM and SidC compete for limiting amounts of PtdIns(4)P on the vacuole. Finally, RNA interference revealed that PtdIns(4)P on LCVs is specifically formed by host PtdIns 4-kinase IIIβ. Thus, *L. pneumophila* exploits PtdIns(4)P produced by PtdIns 4-kinase IIIβ to anchor the effectors SidC and SidM to LCVs.

The Gram-negative pathogen *Legionella pneumophila* is the causative agent of Legionnaires disease, but it evolved as a parasite of various species of environmental predatory protozoa, including the social amoeba *Dictyostelium discoideum* (1, 2). The human disease is linked to the inhalation of contaminated aerosols, followed by replication in alveolar macrophages. To accommodate the transfer between host cells, *L. pneumophila* alternates between replicative and transmissive phases, the regulation of which includes an apparent quorum-sensing system (3–5).

In macrophages and amoebae, *L. pneumophila* forms a replicative compartment, the *Legionella*-containing vacuole (LCV).[3] LCVs avoid fusion with lysosomes (6), intercept vesicular traffic at endoplasmic reticulum (ER) exit sites (7), and fuse with the ER (8–10). The uptake of *L. pneumophila* and formation of LCVs in macrophages and amoebae depends on the Icm/Dot type IV secretion system (T4SS) (11–14). Although more than 100 Icm/Dot substrates ("effector" proteins) have been identified to date, only few are functionally characterized, including effectors that interfere with host cell signal transduction, vesicle trafficking, or apoptotic pathways (15–18).

Two Icm/Dot-translocated substrates, SidM/DrrA (19, 20) and RalF (21), have been characterized as guanine nucleotide exchange factors (GEFs) for the Rho subfamily of small GTPases. These bacterial GEFs are recruited to and activate their targets on LCVs. Small GTPases of the Rho subfamily are involved in many eukaryotic signal transduction pathways and in actin cytoskeleton regulation (22). Inactive Rho GTPases bind GDP and a guanine nucleotide dissociation inhibitor (GDI). The GTPases are activated by removal of the GDI and the exchange of GDP with GTP by GEFs, which promotes the interaction with downstream effector proteins, such as protein or lipid kinases and various adaptor proteins. The cycle is closed by hydrolysis of the bound GTP, which is mediated by GTPase-activating proteins.

SidM is a GEF for Rab1, which is essential for ER to Golgi vesicle transport, and additionally, SidM acts as a GDI displace-

[3] The abbreviations used are: LCV, *Legionella*-containing vacuole; AUC, analytical ultracentrifugation; Dot, defective organelle trafficking; Icm, intracellular multiplication; GEF, guanine nucleotide exchange factor; m.o.i., multiplicity of infection; PI, phosphoinositide; PtdIns, phosphatidylinositol; T4SS, type IV secretion system; PI4K, PtdIns 4-kinase; ER, endoplasmic reticulum; GDI, guanine nucleotide dissociation inhibitor; GDF, GDI displacement factor; RT, reverse transcription; GST, glutathione S-transferase; dsRNA, double-stranded RNA; PH, pleckstrin homology; TGN, *trans*-Golgi network; GFP, green fluorescent protein.

ment factor (GDF) to activate Rab1 (23, 24). The function of SidM is assisted by the Icm/Dot substrate LidA, which also localizes to LCVs. LidA preferentially binds to activated Rab1, thus supporting the recruitment of early secretory vesicles by SidM (19, 20, 23, 25, 26). Another Icm/Dot substrate, LepB (27), contributes to Rab1-mediated membrane cycling by inactivating Rab1 through its GTPase-activating protein function, thus acting as an antagonist of SidM (24).

The Icm/Dot substrate RalF recruits and activates the small GTPase ADP-ribosylation factor 1 (Arf1), which is involved in retrograde vesicle transport from Golgi to ER (21). Dominant negative Arf1 (7, 28) or knockdown of Arf1 by RNA interference (29) impairs the formation of LCVs, as well as the recruitment of the Icm/Dot substrate SidC to the LCV (30).

SidC and its paralogue SdcA localize to the LCV membrane (31), where the proteins specifically bind to the host cell lipid phosphatidylinositol 4-phosphate (PtdIns(4)P) (32, 33). Phosphoinositides (PIs) regulate eukaryotic receptor-mediated signal transduction, actin remodeling, and membrane dynamics (34, 35). PtdIns(4)P is present on the cytoplasmic membrane, but localizes preferentially to the *trans*-Golgi network (TGN), where this PI is produced by an Arf-dependent recruitment of PtdIns(4)P kinase IIIβ (PI4K IIIβ) (36) to promote trafficking along the secretory pathway. Recently, PtdIns(4)P was found to also mediate the export of early secretory vesicles from ER exit sites (37). At present, the *L. pneumophila* effector proteins that mediate exploitation of host PI signaling remain ill defined.

In a nonbiased screen for *L. pneumophila* PI-binding proteins using different PIs coupled to agarose beads, we identified SidM as a major PtdIns(4)P-binding effector. We mapped its PtdIns(4)P binding activity to a novel P4M domain within a 12-kDa C-terminal sequence. SidM constructs, including the P4M domain, were found to be translocated and bind the LCV membrane, where the levels of PtdIns(4)P are controlled by PI4K IIIβ.

EXPERIMENTAL PROCEDURES

Strains and Media—Bacteria and plasmids used in this study are listed in supplemental Table S1. *L. pneumophila* was grown on CYE agar plates or in AYE broth; *Escherichia coli* was cultured in LB medium. Antibiotics were added at the following concentrations: 5 μg/ml chloramphenicol or 50 μg/ml kanamycin for *L. pneumophila* and 30 μg/ml chloramphenicol or 100 μg/ml ampicillin for *E. coli*. The *D. discoideum* wild-type Ax3 strain was grown axenically in HL-5 medium at 23 °C as described, adding 20 μg/ml G418 (32), if required (pSU01). *Drosophila* Kc167 phagocytes were grown at 25 °C in Schneider's medium with 10% heat-inactivated fetal bovine serum (Invitrogen).

Cloning, Recombinant Protein Production, and Purification—Translational N-terminal *gst* or *m45* fusions of *ralF, lidA, sidM,* and fragments of *sidM* were constructed by PCR amplification from chromosomal *L. pneumophila* JR32 DNA using the primers listed in supplemental Table S2. The PCR fragments were cloned into the vectors pGEX-4T-1, pGEX-6P-1, and pCR33, respectively, yielding the plasmids listed in supplemental Table S1. SidC-(1–586)-DL-M9/M13 was produced by cloning PCR fragments generated with oMBglII444fw or oMBglII544fw and

oCR117 into the BglII site of *sidC* and SalI site of pGEX, resulting in the insertion of two additional amino acids (Asp and Leu) between the SidC and SidM fragments. All plasmids were sequenced. Expression of M45 and SidC fusion proteins was verified by Western blot analysis using a monoclonal mouse anti-M45 hybridoma supernatant or an affinity-purified polyclonal rabbit anti-SidC antibody (32), followed by a goat anti-mouse or -rabbit secondary peroxidase-labeled antibody (Sigma). The chromosomal deletions of *ralF* and *sidM* were performed following a protocol described previously (38, 39), and GST fusion proteins were produced as described (32, 33). Details are outlined in the supplemental material.

Pulldown of PtdIns(4)P-binding Proteins—*L. pneumophila* JR32 was grown in AYE medium to an OD_{600} of 3, harvested at 4 °C, washed once in cold W-buffer (10 mM HEPES (pH 7.4), 150 mM NaCl), and lysed with a French press. After addition of 1 mM phenylmethylsulfonyl fluoride, cell debris was removed by centrifugation (10 min, 3,300 $\times$ g), followed by ultracentrifugation (1 h, 155,000 $\times$ g). The amount of soluble protein was estimated using the Bradford assay (Bio-Rad).

For pulldown assays 1–2 ml of lysate containing 10–30 mg of total protein was incubated overnight at 4 °C with 50–100 μl of PI-coated agarose beads (10 pM PtdIns/μl slurry; Echelon). The beads were washed five times in W-buffer. Bound proteins were eluted by adding 20 μl of Laemmli buffer (5 min, 95 °C) and analyzed by SDS-PAGE/Coomassie Brilliant Blue or silver staining. The proteins were digested with trypsin and identified by matrix-assisted laser desorption ionization-tandem mass spectrometry or, alternatively, by liquid chromatography-electrospray ionization-tandem mass spectrometry at the Functional Genomics Center Zurich. Using the same protocol, pulldown assays were also performed with 100 pmol of purified GST fusion protein samples, which were incubated with 50 μl of PtdIns(4)P-coated agarose beads suspended in W-buffer supplemented with 0.25% Nonidet P-40.

Binding of the Different Proteins to Phosphoinositides in Vitro—The binding specificity of different proteins to PIs was tested in a protein-lipid overlay assay (32, 33, 40) using 200 nM GST fusion proteins expressed from pGEX-4T-1 plasmids as detailed in the supplemental material.

Immunofluorescence Microscopy and Quantification of SidC on LCVs—*D. discoideum* was infected with *L. pneumophila* (m.o.i. of 50) and analyzed by fluorescence microscopy as described (4, 32). The bacteria were stained with a monoclonal rhodamine-conjugated rabbit anti-*L. pneumophila* Philadelphia-1 serogroup 1 antibody (m-Tech), and M45-tagged proteins were labeled with a monoclonal mouse anti M45 hybridoma, followed by a Cy5-conjugated goat anti-mouse antibody (The Jackson Laboratories). Alternatively, the bacteria were labeled with a monoclonal mouse anti-*L. pneumophila* Philadelphia-1 serogroup 1 antibody (Santa Cruz Biotechnology), and SidC was stained using an affinity-purified polyclonal rabbit anti SidC antibody (32), followed by a Cy3-conjugated goat anti-mouse and a fluorescein isothiocyanate-labeled anti-rabbit antibody (The Jackson Laboratories).

In other experiments, DsRed-labeled *L. pneumophila* (41) were used to infect calnexin-GFP-producing *D. discoideum*, and SidC on LCVs was visualized by an affinity-purified poly-

clonal rabbit anti-SidC antibody (32) and a secondary goat anti-rabbit Cy5-labeled antibody (The Jackson Laboratories). The amount of SidC was quantified only on calnexin-positive LCVs by determining the fluorescence intensity of the area covering individual LCVs after local background correction using the QuantityOne software (Bio-Rad).

RNA Interference—RNA silencing was performed with *Drosophila* Kc167 phagocytes as described (29, 30). Briefly, 1×10^6 cells/ml were plated in Schneider's medium without serum and incubated for 4 h with dsRNA (20 μg/ml). The transfection process was terminated by adding Schneider's medium with fetal calf serum to a final concentration of 10%, and the cells were incubated for 4–5 days at 25 °C prior to the infections. *Drosophila* genomic DNA and the oligonucleotides listed in supplemental Table S2 were used to amplify by PCR the template DNA containing a T7 promoter for *in vitro* transcription. The PCR products were transcribed *in vitro* into dsRNA using the Megascript RNA kit (Ambion), and the quality of the dsRNA was assessed by gel electrophoresis. Gene silencing by specific dsRNA was confirmed by RT-PCR. To determine effects of gene silencing on the recruitment of SidC to LCVs, 2.5×10^5 Kc167 cells were plated in 24-well dishes containing a coverslip and transfected with dsRNA followed by incubation for 5 days. The cells were infected with *L. pneumophila* (m.o.i. of 50) and incubated at 25 °C for a further 15 min, and SidC-positive LCVs were quantified by immunofluorescence as described (32).

Analytical Ultracentrifugation—To produce full-length SidM for analysis by analytical ultracentrifugation (AUC), the GST-SidM fusion protein was produced, and the GST fragment was cleaved off as described (33). A Beckman XL-I analytical ultracentrifuge using an 8-cell 50Ti rotor was used for the AUC studies. Samples of SidM were prepared in 20 mM Tris-HCl (pH 7.4) containing 100 mM NaCl and 1 mM dithiothreitol and were centrifuged at 20,000, 22,000, and 24,000 rpm for 20 h at 4 °C. The absorbance of the sample was measured at a wavelength of 280 nm throughout the cell. A total of three measurements were taken at 1-h intervals at the end of each run. These measurements were compared to ensure that equilibrium had been reached. Data from each experiment were analyzed using SEDPHAT (42). Parameters for the partial specific volume of the protein were calculated using SEDNTERP (43).

Far-UV Circular Dichroism Spectroscopy—The CD spectra were measured on a Jasco J-810 spectropolarimeter using a 0.02-cm path length cuvette. Protein solutions were prepared in 20 mM Tris-HCl buffer (pH 7.4) including 100 mM NaCl at a concentration of 0.4 mg/ml (5.4, 8.0, 16.8, and 32.5 μM for full-length SidM, M7, M9, and M13, respectively). The scanned wavelength range was 185–300 nm, and the spectra were collected at 20 °C. The secondary structure content was estimated from the CD spectra using the CDSSTR algorithm (44) with reference data set 7 (which contains spectra from 48 proteins, including 5, which are denatured) at the DICHROWEB server (45, 46). The back-calculated spectra and experimental spectra were compared to estimate the normalized root mean square deviation values, which were below 0.1.

Thermofluor Assay—Thermofluor experiments were carried out with a real time PCR machine Mx3005P (Stratagene). The protein was mixed with the fluorescent dye SYPRO Orange (Molecular Probes) in a Thermo-Fast 96-well PCR plate (ABgene), resulting in final protein concentrations of 5 μM. The plate was heated at a rate of 1 °C/min from 25 to 93 °C, and fluorescence was measured in 1 °C increments. Fluorescence was filtered through custom interference excitation (492 nm) and emission (568 nm) filters. The primary data (relative fluorescence intensity *versus* temperature) were fit to standard equations describing protein thermal stability, as described previously (47).

Bioinformatics and Statistical Analysis—Homology searches were performed using the following software packages: BLAST (www.ncbi.nlm.nih), Scansite, PHYRE (protein homology/analogy recognition engine), and ELM (eukaryotic linear motif resource). Prediction of coiled coils was carried out by the Coils Server, and prediction of secondary structure by DomPred and PSIPRED (Protein Structure Prediction Server) (48). For statistical analysis, the one-tailed Student's *t* test was used, considering $p < 0.05$ as significant.

RESULTS

Identification of SidM as a PI-binding Protein—The signaling lipid PtdIns(4)P was recently discovered to be specifically recognized by the Icm/Dot substrate SidC on LCVs (32, 33). To identify additional PI-binding proteins of *L. pneumophila*, we performed pulldown assays using agarose beads coated with individual PIs. Staining of the proteins eluting from washed beads by Coomassie Brilliant Blue revealed large amounts of a protein with an apparent molecular mass of ~75 kDa, which predominantly bound to PtdIns(4)P (Fig. 1*A*). The protein also displayed weaker interactions with PtdIns(3,4)P$_2$. The major PtdIns(4)P interactor was identified by mass spectrometry as the 73-kDa protein SidM, a known Icm/Dot substrate previously characterized as a Rab1 GEF (19, 20).

Upon visualizing proteins eluting from PI-coated beads by silver staining, the 75-kDa protein was also present in eluates from agarose beads coupled to PtdIns(4,5)P$_2$ or PtdIns(3,4,5)P$_3$ (Fig. 1*B*). Thus, the protein appeared to bind PIs phosphorylated at the 4-position. No other proteins specifically binding to any PI were discovered.

The PtdIns(4)P-binding Icm/Dot substrate SidC, which is not similar to SidM in sequence, was expected to also be identified in this screen for PI-binding *L. pneumophila* proteins. Although we did not identify full-length SidC under the above conditions, small amounts of a 50-kDa C-terminal SidC fragment, including the PtdIns(4)P-binding domain "P4C" (33), were retained by PtdIns(4)P-coated agarose beads and identified by mass spectrometry (data not shown).

To determine whether SidC or other *L. pneumophila* proteins bind to PtdIns(4)P-coated agarose beads more efficiently in the absence of SidM, we repeated the pulldown experiments using lysates of an *L. pneumophila* $\Delta sidM$ strain. Whereas in the absence of SidM no protein bound in high amounts to PtdIns(4)P-coated beads, in the absence of SidC only SidM was detected (Fig. 1*C*). These results suggest that SidM is a major PtdIns(4)P-binding protein of *L. pneumophila*.

We also tested whether SidC was not recovered from the enrichment because of proteolytic degradation in *L. pneumo-*
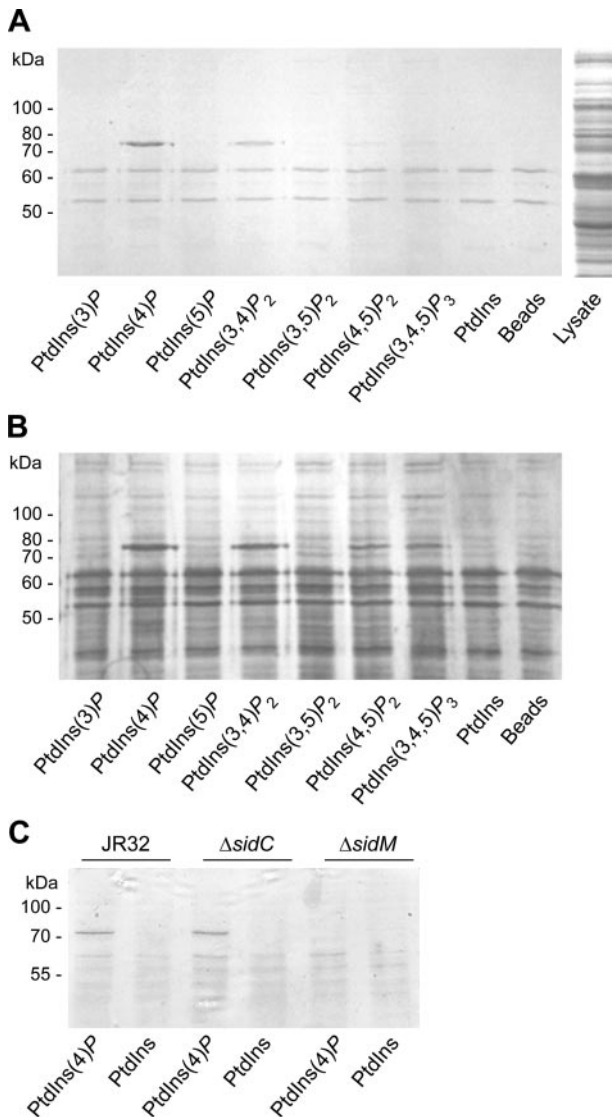
FIGURE 1. **Identification of SidM in a screen for PI-binding *L. pneumophila* proteins.** Pulldown of lysate from *L. pneumophila* wild-type (*A* and *B*), and Δ*sidC* or Δ*sidM* mutant strains (*C*) using agarose beads coated with different PIs or PtdIns. Bacterial proteins retained by washed beads were separated by SDS-PAGE and visualized by staining with Coomassie Brilliant Blue (*A* and *C*) or Silver (*B*). The dominant protein with an apparent molecular mass of ~75 kDa eluting from beads coated with PtdIns(4)P or PtdIns(3,4)P_2 and to a smaller extent from beads coated with PtdIns(4,5)P_2 or PtdIns(3,4,5)P_3 was identified by mass spectrometry as the Rab1 GEF SidM/DrrA.

phila lysates (supplemental Fig. S1). SidC was found to be stable in the absence and in presence of PtdIns(4)P-coated agarose beads for at least 20 h, and thus, proteolysis does not account for the failure to recover significant amounts of SidC under the conditions used.

SidM Specifically Binds to PtdIns(4)P in Vitro—To assess the PI-binding specificity of heterologously produced, purified SidM, we tested binding of an N-terminal GST-SidM fusion protein to agarose beads coated with different PIs. Under the conditions used, the 99-kDa GST-SidM fusion protein bound only to PtdIns(4)P-coated beads, but not to beads coated with any other PIs, PtdIns, or to agarose beads alone (Fig. 2*A*). These results indicate that SidM specifically and directly binds to PtdIns(4)P *in vitro* without requiring any co-factors.
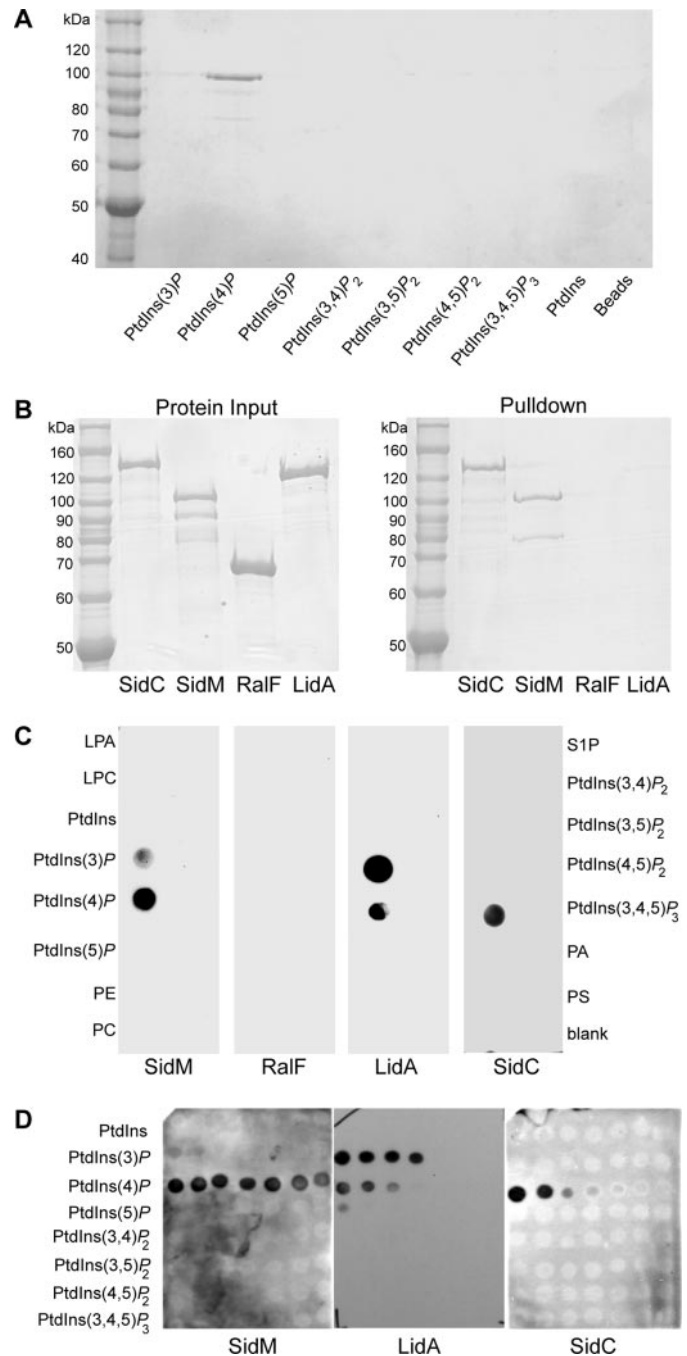

FIGURE 2. **SidM specifically binds to PtdIns(4)P *in vitro*.** SDS gels stained with Coomassie Brilliant Blue of pulldown of affinity-purified GST-SidM with agarose beads coated with different PIs or PtdIns (*A*), or GST-SidM, GST-SidC, GST-RalF, and GST-LidA (3 μg) (*left panel*) and eluate from PtdIns(4)P-coated agarose beads incubated with the GST fusion proteins (*right panel*) (*B*). Protein-lipid overlay assay of 100 pmol (*C*) or serial 2-fold dilutions of the lipids indicated (*D*). The binding of affinity-purified GST fusion proteins to lipids immobilized on nitrocellulose membranes was analyzed using an anti-GST antibody. *LPA*, lysophosphatidic acid; *LPC*, lysophosphocholine; *PE*, phosphatidylethanolamine; *PC*, phosphatidylcholine; *S1P*, sphingosine 1-phosphate; *PA*, phosphatidic acid; *PS*, phosphatidylserine; *PtdIns*, phosphatidylinositol. Similar results were obtained in at least two independent experiments.

SidM was predominantly retained by PtdIns(4)P-coated agarose beads (Fig. 1), even though SidC is also produced by *L. pneumophila* under the conditions used for the screen (33) (supplemental Fig. S1). Possibly, SidM binds to PtdIns(4)P more strongly than SidC. To compare the PtdIns(4)P affinities of
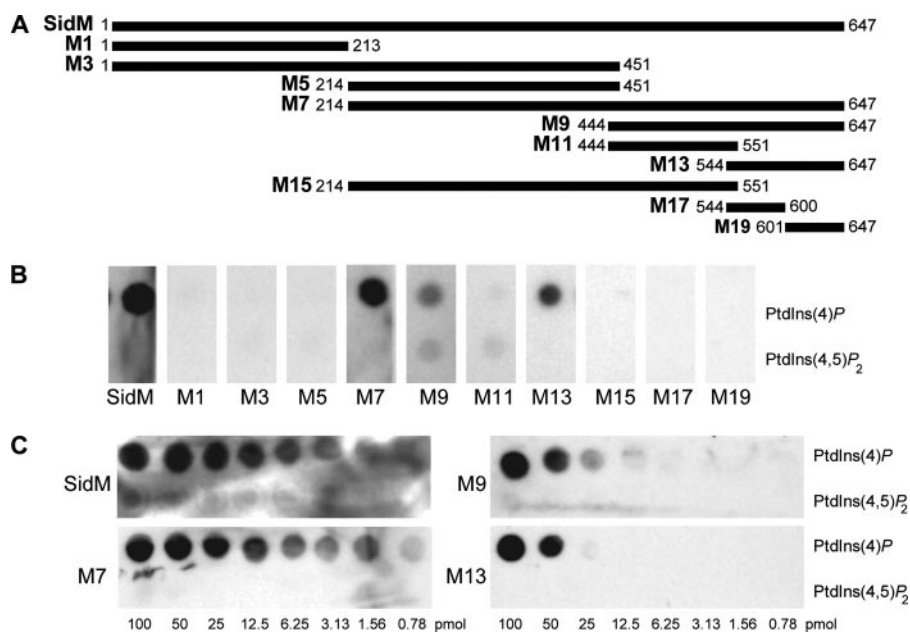
FIGURE 3. **Identification of the PtdIns(4)P-binding domain of SidM.** *A,* SidM fragments fused to GST were affinity-purified and used in protein-lipid overlay assay to test binding to 100 pmol (*B*) or serial 2-fold dilutions of PtdIns(4)P and PtdIns(4,5)P$_2$ spotted onto nitrocellulose membranes (*C*).

to PtdIns(4)P by protein-lipid overlay assays (Fig. 3*A*). Full-length SidM (73 kDa) and the C-terminal fragments M7 (49 kDa, SidM-(214–647)), M9 (23 kDa, SidM-(444–647)), and M13 (12 kDa, SidM-(544–647)) bound to PtdIns(4)P but not to PtdIns(4,5)P$_2$, which was used as a negative control (Fig. 3*B*). M13 was the smallest PtdIns(4)P-binding fragment identified, and upon further cleavage into the N- and C-terminal fragments M17 and M19, PtdIns(4)P binding activity was completely lost. The M13 PtdIns(4)P-binding domain does not show any homology to the PtdIns(4)P-binding pleckstrin homology (PH) domain of the eukaryotic adaptor protein FAPP1 (40), the P4C domain of *L. pneumophila* SidC (33), or any other prokaryotic or eukaryotic PI-binding protein. Thus, we termed this novel module the "P4M" (PtdIns4P binding of SidM/DrrA) domain.

The N-terminal fragments of SidM, M1, and M3, or the internal fragments M5, M11, and M15, did not bind to PtdIns(4)P (Fig. 3). Notably, only the 49-kDa fragment M7, comprising amino acid residues 214–647 of SidM, bound PtdIns(4)P as efficiently as full-length SidM. The affinity of the smaller fragments M9 (23 kDa, SidM-(444–647)) and M13 (12 kDa, SidM-(544–647)) appeared to be ~50-fold reduced, as estimated by a 2-fold dilution series of PtdIns(4)P (Fig. 3*C*). We suggest that this may be attributed to the lack of predicted coiled coil regions or other structurally stabilizing elements in these fragments.

Structural Analysis of SidM and Fragments—AUC of purified full-length SidM revealed a single species of 71,282 ± 586 Da, indicating a homogeneous monomeric state (Fig. 4*A*). Further structural analysis of full-length SidM and the fragments M7, M9, and M13 by CD revealed that the α-helical content of the full-length protein and M7 fragment was similar and ~67 or 71%, respectively (Fig. 4*B* and Table 1), matching the predicted secondary structure. In contrast, the M9 and M13 fragments were found by CD spectroscopy to adopt only ~48 and 59% α-helical structure, compared with predictions of 69 or 73%, respectively. These results suggest that the M9 and M13 fragments are structurally less stable, a finding that is reinforced by the poorly resolved NMR spectra of ^{15}N-labeled M13 protein (data not shown). As a corollary, we suggest that the entire PtdIns(4)P binding structural domain of SidM includes residues N-terminal to residue 444, which are present in the M7 construct. In agreement with this notion, the M9 and M13 fragments were found by Thermofluor assays to lack a thermal unfolding transition typical of a globular fold, whereas the longer constructs revealed an unfolding transition between 65 and 72 °C (Fig. 4*C*). This instability of the M9 and M13 SidM fragments likely accounts for their apparent 50-fold reduced affin-

Icm/Dot substrates localizing to LCVs, we directly compared binding of the corresponding GST fusion proteins in pulldown assays. Agarose beads coated with PtdIns(4)P were incubated with equal amounts of the purified GST fusion proteins of SidC, SidM, RalF, and LidA. Proteins retained by the beads were separated by SDS-PAGE and visualized by Coomassie Brilliant Blue staining (Fig. 2*B*). Similar amounts of purified GST-SidC and GST-SidM eluted from the beads, indicating that the affinities of the two different effectors to PtdIns(4)P are comparable. Compared with the amount of protein applied, ~20% of GST-SidC or GST-SidM eluted from the beads. In contrast, GST-RalF was not retained by PtdIns(4)P-coated agarose beads, and only a very faint band was observed for GST-LidA eluting from the beads.

Next, we tested binding of purified GST fusion proteins of SidM, RalF, LidA, and SidC to PIs and other lipids immobilized on nitrocellulose membranes (Fig. 2*C*). The Rab1 GEF SidM preferentially bound to PtdIns(4)P and weakly also to PtdIns(3)P. In contrast, the Arf1 GEF RalF did not bind to any PIs or other lipids on the membrane, suggesting that *L. pneumophila* produces distinct classes of GEFs that localize to LCVs either PI-dependently or PI-independently. Interestingly, the SidM auxiliary protein LidA preferentially bound to PtdIns(3)P but also significantly to PtdIns(4)P. Finally, as observed previously, SidC specifically bound PtdIns(4)P. These results were confirmed using PI array nitrocellulose membranes, onto which the PIs are spotted in 2-fold dilution series (Fig. 2*D*). On these arrays SidM and SidC specifically bound to PtdIns(4)P, whereas LidA showed a more relaxed PI-binding specificity and preferentially bound to PtdIns(3)P but also weakly to PtdIns(4)P.

Identification of the PtdIns(4)P-binding Domain of SidM—To map the PtdIns(4)P-binding domain of SidM, we constructed N-terminal fusions of GST with fragments of SidM of different lengths and visualized binding of the fusion proteins
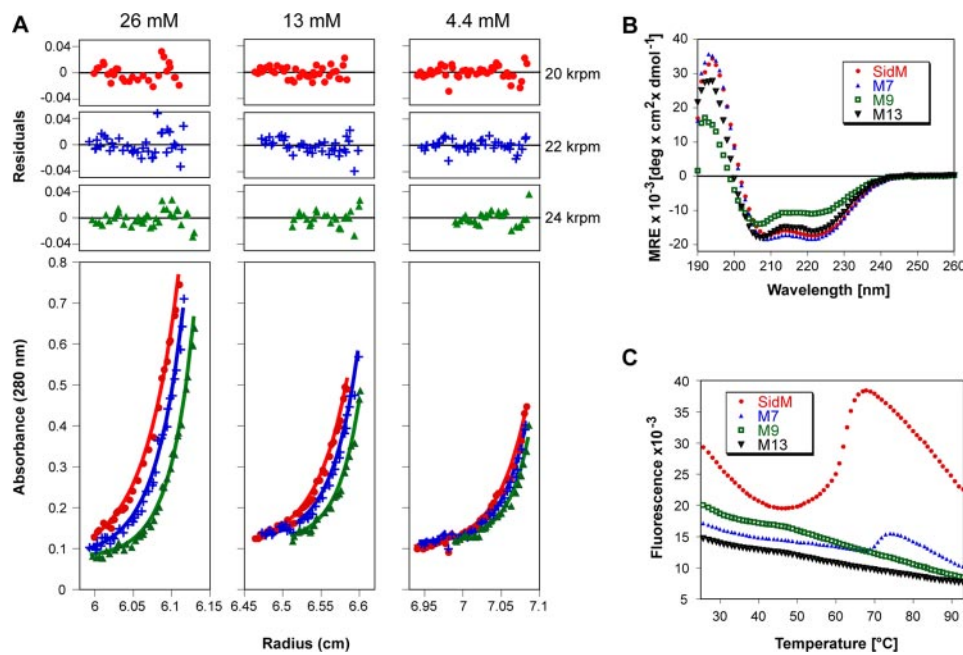
FIGURE 4. **Structural analysis of SidM and fragments.** *A,* sedimentation equilibrium analysis of full-length SidM revealed an ~71-kDa species corresponding to a monomeric state. *B,* far-UV CD spectra of the full-length protein SidM (*red*) and the fragments M7 (*blue*), M9 (*green*), and M13 (*black*). The signal unit is converted into mean residue ellipticity (*MRE*). The helical structure is evidenced by strong negative ellipticities at around 220 and 208 nm. *C,* thermofluor assay for the full-length SidM protein and the fragments M7, M9, and M13. The estimated unfolding transition temperatures of full-length SidM and the fragment M7 were 62.3 and 71.4 °C, respectively, whereas the M9 and M13 fragments did not display cooperative unfolding transitions.

TABLE 1

Secondary structure contents of SidM and fragments estimated by CDSSTR

Fragment	α^a	β^a	Turn	Disordered
	%	%	%	%
SidM	67 (67.0)	6 (3.4)	12	15
M7	71 (71.7)	9 (3.0)	10	10
M9	48 (68.8)	24 (4.4)	10	18
M13	59 (73.1)	8 (5.8)	12	20

^{a} Values in parentheses indicate predicted α-helix or β-strand contents from secondary structure prediction using DomPred.

ity for PtdIns(4)P, compared with full-length SidM and the M7 fragment (Fig. 3*C*).

C-terminal Fragments of SidM Localize to LCVs in Vivo—In vitro, SidM specifically binds to PtdIns(4)P (Fig. 2), a compound that has been identified as a lipid component of LCVs (32). We used *D. discoideum* to address the question of whether SidM not only localizes to the LCV membrane in infected macrophages (19, 20) but also in amoebae, and whether N-terminal PtdIns(4)P-binding fragments of SidM are still translocated by the Icm/Dot T4SS and bind to the LCV membrane. To this end, we produced M45-tagged SidM and fragments thereof in the wild-type *L. pneumophila* strain JR32, infected the amoebae, and analyzed the localization by immunofluorescence microscopy (Fig. 5*A*). Full-length M45-SidM as well as M45-SidC, used as a positive control (33), were translocated and bound to LCV membranes in *D. discoideum* amoebae, as expected. The SidM fragment M45-M7, including the P4M domain but lacking a 24-kDa N-terminal fragment, was also translocated into *D. discoideum* and bound to LCV membranes, indicating that SidM possesses a C-terminal translocation signal. Approximately, 66% of calnexin-positive LCVs also stained positive for

M45-M7. The translocation of M45-M7 required a functional Icm/Dot T4SS and did not occur in a $\Delta icmT$ mutant strain.

In a similar way, we attempted to analyze translocation and LCV binding of smaller SidM fragments. However, using an anti-M45 antibody we neither detected translocation of M45-M9 or M45-M13, nor production of these fragments in lysates of *L. pneumophila* (data not shown). Presumably, these small fragments are not sufficiently stable when produced in the bacteria, as indicated by the Thermofluor experiments described above (Fig. 4*C*). To possibly stabilize the small SidM fragments, we constructed fusion proteins with a 67-kDa N-terminal fragment of SidC (SidC-(1–586)) that does not bind to PtdIns(4)P *in vitro* and is not translocated to LCV membranes *in vivo* (33). In addition, this strategy allowed the use of a polyclonal anti-SidC antibody, which is more sensitive than the monoclonal anti M45 antibody (data not shown). Whereas SidC-(1–586)-M13 was still not detectable by Western blot, SidC-(1–586)-M9 was produced by *L. pneumophila*, although at a much reduced level (~4%) compared with full-length SidC (data not shown). Upon infection of *D. discoideum* with an *L. pneumophila* $\Delta sidC$-$sdcA$ mutant strain producing SidC-(1–586)-M9, the fusion protein was detected on LCVs by immunofluorescence using an anti-SidC antibody (Fig. 5*B*). This result indicates that the 23-kDa SidM fragment M9 is translocated into *D. discoideum* and binds to LCVs, in agreement with the notion that the 12-kDa N-terminal P4M domain anchors SidM to the LCV membrane. As observed previously, full-length SidC but not SidC-(1–608) was translocated and bound to LCVs (33).

Competition of SidM and SidC for PtdIns(4)P on LCVs— SidM was the predominant protein bound by PtdIns(4)*P*-coated agarose beads in *L. pneumophila* lysates (Fig. 1), suggesting that this effector is a major PtdIns(4)P-binding protein. As a corollary, higher amounts of other *L. pneumophila* PtdIns(4)P-binding proteins are predicted to bind to LCVs in the absence of SidM. To test this hypothesis, we quantified on LCVs harboring different *L. pneumophila* strains the Icm/Dot substrate SidC, which binds to PtdIns(4)P *in vitro* with an affinity comparable with SidM (Fig. 2).

The amount of SidC on LCVs was determined by immunofluorescence after infecting calnexin-GFP producing *D. discoideum* with *L. pneumophila* wild-type, $\Delta sidM$, $\Delta sidC$-$sdcA$, or $\Delta ralF$ mutant strains (Fig. 6*A*). In agreement with the above notion, the median fluorescence intensity of SidC bound to LCVs significantly increased ~1.5 times in the absence of SidM ($p < 10^{-4}$), whereas the absence of the PI-independent GEF
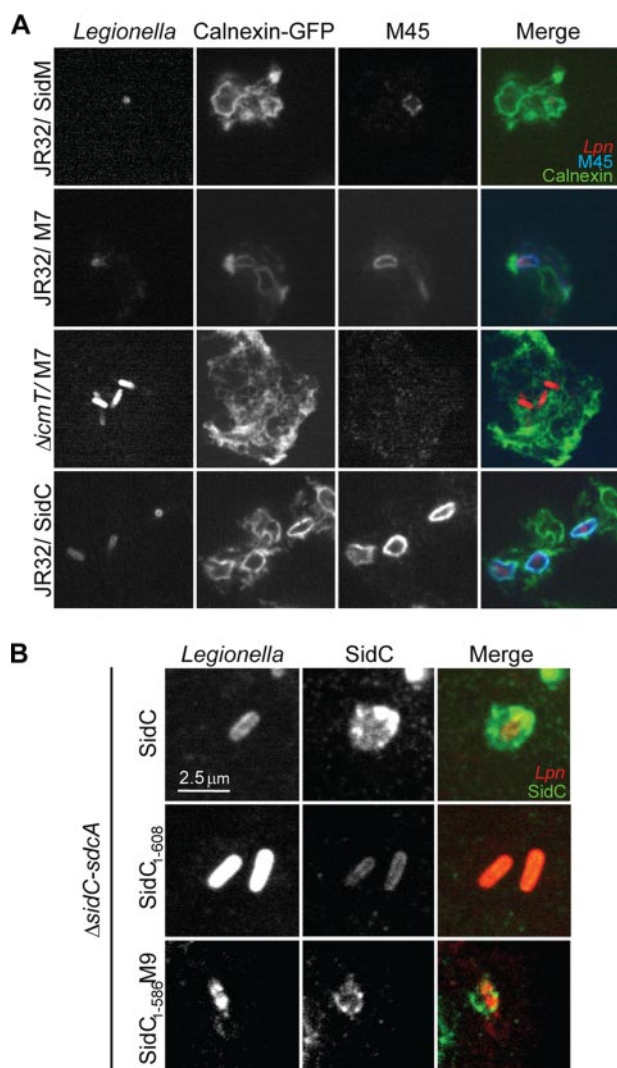
FIGURE 5. **C-terminal fragments of SidM localize to LCVs.** *A,* confocal laser scanning micrographs of calnexin-GFP-labeled *D. discoideum* Ax3 (*green*), infected at an m.o.i. of 50 for 1 h with *L. pneumophila* labeled with a serogroup 1-specific antibody (*red*) and immunostained for M45-SidM, M45-M7, and M45-SidC with an anti-M45 antibody (*blue*). *B, D. discoideum* was infected at an m.o.i. of 50 for 1 h with *L. pneumophila* Δ*sidC-sdcA* harboring plasmid pCR34 (M45-SidC), pCR52 (M45-SidC-(1–608)), or pEB216 (SidC-(1–586))-M9) and immunostained using antibodies against *L. pneumophila* serogroup 1 (*red*) and SidC (*green*). The experiments were reproduced three (*A*) or two (*B*) independent times with similar results.

RalF did not affect binding of SidC to LCVs (Fig. 6*B*). The assay was specific for SidC, because upon infection of *D. discoideum* with an *L. pneumophila* strain lacking SidC and its paralogue SdcA, only background fluorescence was measured on LCVs. Moreover, whereas the Δ*sidC-sdcA* mutant strain did not produce any SidC as expected, the levels of SidC produced by wild-type, Δ*sidM*, and Δ*ralF L. pneumophila* were the same (supplemental Fig. S1), ruling out that the different amounts of SidC on LCVs were because of different production levels of SidC in the bacterial strains.

In addition, we characterized LCVs harboring *L. pneumophila* wild-type, Δ*sidM*, Δ*sidC-sdcA,* or Δ*ralF* mutant strains with regard to the acquisition of the ER marker calnexin. Whereas LCVs harboring the Δ*sidC-sdcA* strain were defective for calnexin acquisition as described previously (33), LCVs con-

taining the Δ*sidM* or Δ*ralF* strains accumulated calnexin to the same extent as wild-type LCVs, indicating that trafficking and composition of these LCVs are similar (data not shown).

To confirm the findings obtained with SidC translocated by *L. pneumophila*, we ectopically produced the PtdIns(4)P-binding probe GFP-SidC$_{P4C}$ in *D. discoideum* and quantified free PtdIns(4)P on LCVs (Fig. 6*C*) (33). Using this probe, we observed that the GFP fluorescence intensity on LCVs containing either an *L. pneumophila* Δ*sidM* or Δ*sidC-sdcA* mutant strain significantly increased ~1.5 times ($p < 3 \times 10^{-2}$), compared with LCVs harboring wild-type *L. pneumophila* or a strain lacking the PI-independent GEF RalF (Fig. 6*D*). Hence, the results obtained with SidC endogenously produced by *L. pneumophila* and GFP-SidC$_{P4C}$ ectopically produced by *D. discoideum* are consistent. In summary, our findings indicate that SidM as well as SidC and SdcA are major PtdIns(4)P-binding effector proteins that compete for PtdIns(4)P-binding sites on LCV membranes.

Production of PtdIns(4)P on LCVs Involves PI4K IIIβ— PtdIns(4)P is synthesized from PtdIns, which in metazoan cells is catalyzed by several PI4Ks. These enzymes preferentially localize to different subcellular compartments: PI4K IIα/β to the TGN, endosomes, and plasma membrane; PI4K IIIα to the ER, plasma membrane, and nucleus; and PI4K IIIβ to the Golgi, respectively (34, 49). In the TGN, PtdIns(4)P is formed by PI4K IIIβ upon recruitment by Arf1 (36).

To resolve whether a specific PI4K controls the levels of PtdIns(4)P on LCVs, we knocked down the respective kinases by RNA interference in *Drosophila* Kc167 phagocytes, which are permissive for intracellular replication of *L. pneumophila* (29). Although mRNA of PI4K IIIβ, PI4K IIIα, and PI4K IIα was readily amplified by RT-PCR in control cells, dsRNA oligonucleotides specific against individual PI4Ks reduced gene expression to a level not detectable by RT-PCR (supplemental Fig. S2).

After infection of the *Drosophila* phagocytes with *L. pneumophila*, we quantified the amount of SidC on LCVs (Fig. 7*A*). Using this assay, we found that the accumulation of SidC on LCVs was impaired upon depletion of PI4K IIIβ, but not PI4K IIIα or PI4K IIα (Fig. 7*B*). Depletion of PI4K IIIβ decreased the number of SidC-positive LCVs by ~4.5-fold, indicating that this PI4K controls the level of PtdIns(4)P on LCVs, which in turn is bound by SidC (and other PtdIns(4)P-binding effectors). Because the depletion of PI4K IIIβ did not impair intracellular replication of *L. pneumophila* (data not shown), PtdIns(4)P-dependent recruitment of SidC (and other PtdIns(4)P-binding effectors) is not rate-limiting for intracellular replication. This result corresponds to the finding that *L. pneumophila* Δ*sidC-sdcA* (31, 33) or Δ*sidM* (19, 20) mutant strains grow at wild-type rate.

DISCUSSION

PI-binding L. pneumophila Effector Proteins—L. pneumophila forms a replicative vacuole within phagocytes by means of the Icm/Dot T4SS and more than 100 effector proteins, most of which have not been functionally characterized to date. We recently discovered that the Icm/Dot substrate SidC specifically binds to PtdIns(4)P *in vitro* (32). SidC is a bi-functional effector, which anchors to LCVs by binding to PtdIns(4)P via its
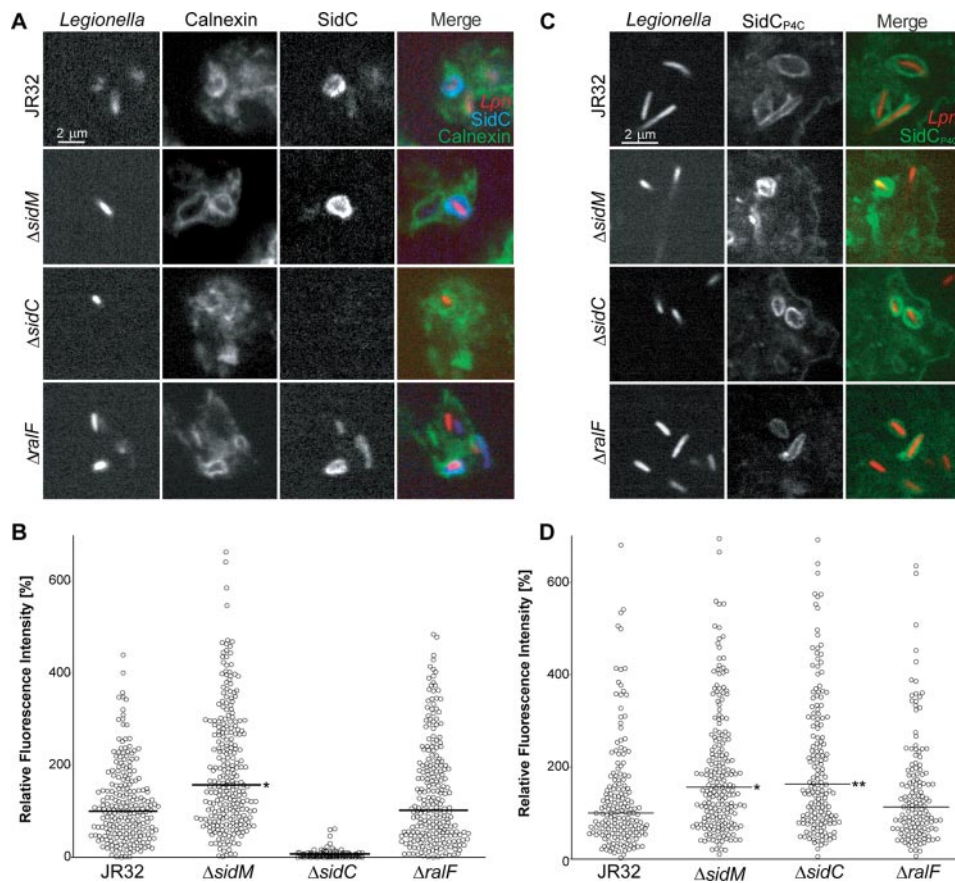
FIGURE 6. **Competition of SidM and SidC for PtdIns(4)P on LCVs.** *A,* confocal laser scanning micrographs; *B,* dot plot of SidC fluorescence on LCVs in calnexin-GFP-producing *D. discoideum* Ax3 (*green*), infected with DsRed-labeled *L. pneumophila* (*red*) wild-type JR32, Δ*sidM*, Δ*ralF*, or Δ*sidC-sdcA* and immunostained for SidC (*blue*). The data and the median (*, $p < 10^{-4}$) are derived from three independent experiments ($n > 200$), which were normalized to the median of SidC fluorescence of wild-type JR32. *C,* confocal laser scanning micrographs; *D,* dot plot of GFP-SidC$_{P4C}$ fluorescence (*green*) on LCVs in *D. discoideum* Ax3 harboring the plasmid pSU01, infected with DsRed-labeled *L. pneumophila* (*red*) wild-type JR32, Δ*sidM*, Δ*ralF*, or Δ*sidC-sdcA*. The data are combined from three independent experiments ($n > 143$), each normalized to the median fluorescence obtained with JR32 (*, $p < 3 \times 10^{-2}$; **, $p < 5 \times 10^{-4}$).

that of GST-SidM (Fig. 2*B*), suggesting that the intrinsic affinity of the two purified effector proteins for PtdIns(4)P is similar.

To explain the paradox posed by the PtdIns(4)P activities of SidC, we propose that the P4C PtdIns(4)P-binding domain of SidC is masked, either "in *cis*" by one of its own domains or "in *trans*" by another protein. Supporting the first notion, we found that in the absence of a 70-kDa N-terminal fragment the 20-kDa P4C fragment or a 36-kDa C-terminal fragment seem to bind PtdIns(4)P with higher affinity (33). Alternatively or additionally, SidC might be complexed by other *L. pneumophila* proteins in the bacterial cytoplasm (lysate), thus preventing binding to PtdIns(4)P. Obvious candidates for such proteins are IcmS and IcmW, which constitute a putative chaperone complex within the bacterial cell, necessary for Icm/Dot-mediated translocation of a subset of effectors (50, 51). Translocation of SidC is significantly decreased in either *L. pneumophila* Δ*icmS* or Δ*icmW* single mutant strains and occurs as much as 10-fold less efficiently in the Δ*icmS-icmW* double mutant (52). In addition to SidC, the IcmS-IcmW complex might bind other *L. pneumophila* effector proteins in the cytoplasm, thus preventing their interaction with PtdIns(4)P in bacterial lysates.

Interestingly, *L. pneumophila* produces at least two families of PI-binding effector proteins, which display distinct preferences for PIs. Whereas SidM (Fig. 2) and SidC (32, 33) almost exclusively bind PtdIns(4)P, the Icm/Dot substrate LidA preferentially binds PtdIns(3)P but also PtdIns(4)P (Fig. 2), and the effector LpnE (53, 54) selectively binds PtdIns(3)P (55). Accordingly, the specificity of *L. pneumophila* PI-binding effectors seems to be strongly biased toward mono-phosphorylated PIs, in particular PtdIns(4)P (SidC and SidM) and PtdIns(3)P (LidA and LpnE). Because the cellular concentration of PtdIns(4)P is much higher than PtdIns(3)P, PtdIns(4)P might actually be the dominant ligand for LidA *in vivo*. This notion is in agreement with the function of LidA as an auxiliary protein for the PtdIns(4)P-binding effector SidM.

PtdIns(4)P-binding Domain of SidM—The minimal PtdIns(4)P-binding domain of SidM was mapped to the 12-kDa C-terminal M13 fragment and termed the P4M domain (Fig. 3). This domain includes amino acids 544–647 and thus does not overlap with functional domains of SidM described previously. A number of functions of SidM have been assigned to amino acids

C-terminal P4C domain and promotes the interaction with ER via its N-terminal domain (33). Based on these findings, we performed an unbiased screen using agarose beads coupled to different PIs to discover other PI-binding *L. pneumophila* proteins. Thus, we identified the Rab1 GDF/GEF SidM as a major PtdIns(4)P-binding effector (Fig. 1). This finding represents a novel link between the exploitation of PIs and the modulation of host GTP metabolism by pathogenic bacteria.

SidM eluted as the predominant protein from PtdIns(4)P-coated agarose beads, and no other proteins seemed to be strongly retained by any PI-coated beads. Notably, a C-terminal fragment of SidC was identified in the eluate of PtdIns(4)P-coated beads, but the effector was apparently not retained in high amounts by the beads. Therefore, SidM might be either produced at lower levels compared with SidM, be less stable, or bind less strongly to PtdIns(4)P-coated agarose beads. In lysates of *L. pneumophila* prepared like the samples used for the screen, SidC was readily detected by Western blot (33) and stable for at least 20 h (supplemental Fig. S1), indicating that SidC is indeed produced and not proteolytically degraded under these conditions. Moreover, the binding affinity to PtdIns(4)P of recombinant GST-SidC was comparable with
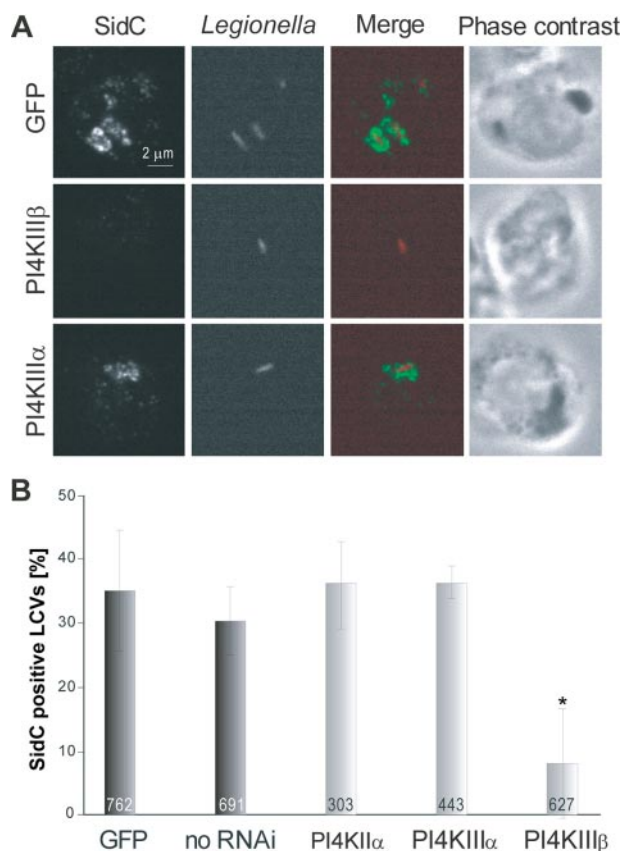
FIGURE 7. Production of PtdIns(4)P on LCVs involves PI4K IIIβ. *A,* confocal laser scanning micrographs of *Drosophila* Kc167 phagocytes treated with the dsRNA indicated and infected at an m.o.i. of 50 for 15 min with DsRed-labeled wild-type *L. pneumophila* (*red*). Recruitment of the PtdIns(4)P-binding Icm/Dot substrate SidC was analyzed by immunofluorescence microscopy using an affinity-purified antibody against SidC (*green*). *Bar,* 2 μm. *B,* quantification of SidC recruitment to LCVs. Means and standard deviations of three independent experiments are shown ($n = 303–762$, *, $p < 2 \times 10^{-2}$). *RNAi,* RNA interference.

317–545, such as binding of the Rab1 GTPase, as well as the GEF and GDF activities (20). The P4M domain does not share homology with the PtdIns(4)P-binding domain P4C of SidC (33) or with eukaryotic PtdIns(4)P recognition folds, including the PH domain of FAPP1 (40), the PX domain of Bem1p (56), and the VHS domain of Gga2p (57). However, the SidM topology may resemble the BAR/IMD domains, which are helical bundles that also bind PIs and induce membrane curvature (58). Some BAR domains form oligomers on membranes, and therefore we speculate that a PtdIns(4)P- and membrane-dependent oligomerization of SidM might contribute to the higher affinity toward PtdIns(4)P of the full-length protein compared with the M9 and M13 (P4M) fragments (Fig. 3).

The apparent PtdIns(4)P affinity of the full-length SidM or the 49-kDa M7 fragment is ~50-fold higher than that of the 12-kDa P4M domain (or the 23-kDa M9 fragment) (Fig. 3). This stronger interaction is possibly caused by the greater structural stability of the longer forms, as evidenced by the CD and Thermofluor experiments (Fig. 4, *B* and *C*). Indeed, several coiled coils are predicted in the N-terminal 400 residues of SidM and are missing in the shorter constructs. However, this region does not appear to mediate obligatory homo-oligomerization of

SidM, as the full-length protein is monomeric (Fig. 4*A*). The M3, M5, and M15 fragments are not directly involved in binding of PtdIns(4)P; however, these portions of SidM might contribute to stabilizing the P4M domain, thereby increasing its affinity for PtdIns(4)P. In contrast to SidM, the P4C domain of SidC, as well as its 36-kDa C-terminal fragment, bound PtdIns(4)P more tightly than the full-length effector protein (33). Thus, whereas the SidC P4C domain is a suitable probe for the analysis of PtdIns(4)P in cell biological and biochemical experiments, only full-length SidM or the M7 fragment are recommended as stable PtdIns(4)P-binding tools.

Both the P4M and P4C domains are located in the C termini of the corresponding effector proteins. However, although the 12-kDa P4M domain constitutes the very C terminus of SidM, the 20-kDa P4C domain lies 16-kDa upstream of the C terminus of SidC. The C-terminal SidM fragment M7 and the fusion protein SidC-(1–586)-M9 were translocated by Icm/Dot-proficient *L. pneumophila* into *D. discoideum* and bound to LCV membranes (Fig. 5). This result suggests that SidM contains a C-terminal translocation signal, similar to the Icm/Dot substrates SidC (33), RalF (59), SdhA, and its paralogue SidH (60) as well as SidG (52). Moreover, SidM features an isoleucine at position −4 in relation to the C terminus, which is in agreement with the finding that a hydrophobic amino acid at position −3 or −4 is critical for Icm/Dot-dependent secretion (59).

Different Classes of L. pneumophila GEFs—Two different kinds of GEFs can be classified in *L. pneumophila* based on the nature of their PI interactions. Whereas the Rab1 GEF SidM localizes to LCVs (19, 20) by binding to PtdIns(4)P, the Arf1 GEF RalF localizes to LCVs (21) very likely independently of PIs, because it does not bind to PIs *in vitro* (Fig. 2*C*). Both GEFs recruit host cell GTPases to LCVs. SidM recruits and activates the small GTPase Rab1 (19, 20), which is present in the host cytoplasm in its inactive state bound to a GDI. Rab-GDI complexes are recognized by a specific GDF, and after GDI dissociation Rab-GDP becomes membrane-associated before being activated by a membrane-bound GEF (61). In contrast, the small GTPase Arf1 itself is able to associate with PtdIns(4,5)P_2, and this in turn appears to promote a conformational change required for association with its GEF (62). These distinct features of the GTPases may account for the different characteristics of the two *L. pneumophila* GEFs SidM and RalF with regard to PI binding.

Binding to and Production of PtdIns(4)P on LCVs—PtdIns(4)P is present on LCVs (32), and therefore, SidM as well as SidC likely anchor to the vacuole via this PI. Even though these *L. pneumophila* effectors directly and selectively bound to PtdIns(4)P *in vitro*, we cannot rule out that binding on LCVs involves a co-receptor. The mammalian four-phosphate-adaptor proteins FAPP1 and FAPP2 interact with PtdIns(4)P on the Golgi through their PH domains, and additionally bind the GTP-bound form of the small GTPase Arf1 (63). *L. pneumophila* recruits and activates Arf1 at the LCV membrane by means of the Icm/Dot substrate RalF (21), and depletion of Arf1 by RNA interference abolishes binding of SidC to LCVs (30). Therefore, analogously to the FAPPs on the Golgi, SidM and SidC might bind to PtdIns(4)P in the context of activated Arf1 on LCVs. On the other hand, depletion or inhibition of the

pleiotropic small GTPase Arf1 prevents the formation of replication-permissive LCVs altogether (7), and thus, a drastically altered vacuole membrane composition might nonspecifically reduce the amounts of bound SidC.

Using RNA interference in *Drosophila* phagocytes, we showed that PI4K IIIβ but not PI4K IIIα or PI4K IIα promote the binding of SidC to LCVs (Fig. 7). It is currently not clear whether and how PI4K IIIβ accumulates on LCVs. PI4K IIIβ is recruited to the TGN by Arf1 (36), and therefore, the PI4K might localize to LCVs by direct fusion with the TGN or with other cellular compartments enriched in PI4K IIIβ. Alternatively, recruitment of cytoplasmic Arf1 to LCVs by *L. pneumophila* RalF (21) might lead to an accumulation of PI4K IIIβ. However, in the absence of RalF, the amount of SidC or ectopically expressed GFP-SidC$_{P4C}$ on LCVs in *D. discoideum* was not affected (Fig. 6), indicating that the pathway involving Arf1 and PI4K IIIβ is probably not relevant on LCVs.

In contrast to the deletion of *ralF*, deletion of *sidM* significantly increased the amount of SidC on LCVs (Fig. 6). SidM recruits Rab1 to LCVs (19, 20), yet knockdown of Rab1 in *Drosophila* cells did not affect the levels of SidC on LCVs (30). Therefore, the increased amounts of SidC on LCVs harboring *L. pneumophila* Δ*sidM* mutant bacteria are likely caused by increased levels of free PtdIns(4)P, which on LCVs harboring wild-type *L. pneumophila* is bound by SidM. In agreement with this notion, the amount of the ectopically produced PtdIns(4)P probe SidC$_{P4C}$, significantly increased on LCVs harboring either *L. pneumophila* Δ*sidM* or Δ*sidC-sdcA* (Fig. 6D). Together, these results support the general concept that *L. pneumophila* exploits specific host PIs to anchor effector proteins to the LCV membrane, and furthermore, our findings suggest that SidM and SidC are (the) major PtdIns(4)P-binding effectors, which compete for free PtdIns(4)P-binding sites on LCVs.

REFERENCES

1. Fields, B. S., Benson, R. F., and Besser, R. E. (2002) *Clin. Microbiol. Rev.* **15,** 506–526
2. Hilbi, H., Weber, S. S., Ragaz, C., Nyfeler, Y., and Urwyler, S. (2007) *Environ. Microbiol.* **9,** 563–575
3. Spirig, T., Tiaden, A., Kiefer, P., Buchrieser, C., Vorholt, J. A., and Hilbi, H. (2008) *J. Biol. Chem.* **283,** 18113–18123
4. Tiaden, A., Spirig, T., Weber, S. S., Brüggemann, H., Bosshard, R., Buchrieser, C., and Hilbi, H. (2007) *Cell. Microbiol.* **9,** 2903–2920
5. Tiaden, A., Spirig, T., Carranza, P., Brüggemann, H., Riedel, K., Eberl, L., Buchrieser, C., and Hilbi, H. (2008) *J. Bacteriol.* **190,** 7532–7547
6. Horwitz, M. A. (1983) *J. Exp. Med.* **158,** 2108–2126
7. Kagan, J. C., and Roy, C. R. (2002) *Nat. Cell Biol.* **4,** 945–954
8. Horwitz, M. A. (1983) *J. Exp. Med.* **158,** 1319–1331
9. Robinson, C. G., and Roy, C. R. (2006) *Cell. Microbiol.* **8,** 793–805
10. Lu, H., and Clarke, M. (2005) *Cell. Microbiol.* **7,** 995–1007
11. Hilbi, H., Segal, G., and Shuman, H. A. (2001) *Mol. Microbiol.* **42,** 603–617
12. Segal, G., Purcell, M., and Shuman, H. A. (1998) *Proc. Natl. Acad. Sci. U. S. A.* **95,** 1669–1674
13. Vogel, J. P., Andrews, H. L., Wong, S. K., and Isberg, R. R. (1998) *Science* **279,** 873–876
14. Segal, G., Feldman, M., and Zusman, T. (2005) *FEMS Microbiol. Rev.* **29,** 65–81
15. Brüggemann, H., Cazalet, C., and Buchrieser, C. (2006) *Curr. Opin. Microbiol.* **9,** 86–94
16. Hilbi, H. (2006) *Cell. Microbiol.* **8,** 1697–1706
17. Ninio, S., and Roy, C. R. (2007) *Trends Microbiol.* **15,** 372–380
18. de Felipe, K. S., Glover, R. T., Charpentier, X., Anderson, O. R., Reyes, M., Pericone, C. D., and Shuman, H. A. (2008) *PLoS Pathog.* **4,** e1000117
19. Machner, M. P., and Isberg, R. R. (2006) *Dev. Cell* **11,** 47–56
20. Murata, T., Delprato, A., Ingmundson, A., Toomre, D. K., Lambright, D. G., and Roy, C. R. (2006) *Nat. Cell Biol.* **8,** 971–977
21. Nagai, H., Kagan, J. C., Zhu, X., Kahn, R. A., and Roy, C. R. (2002) *Science* **295,** 679–682
22. Jaffe, A. B., and Hall, A. (2005) *Annu. Rev. Cell Dev. Biol.* **21,** 247–269
23. Machner, M. P., and Isberg, R. R. (2007) *Science* **318,** 974–977
24. Ingmundson, A., Delprato, A., Lambright, D. G., and Roy, C. R. (2007) *Nature* **450,** 365–369
25. Conover, G. M., Derre, I., Vogel, J. P., and Isberg, R. R. (2003) *Mol. Microbiol.* **48,** 305–321
26. Derre, I., and Isberg, R. R. (2005) *Infect. Immun.* **73,** 4370–4380
27. Chen, J., de Felipe, K. S., Clarke, M., Lu, H., Anderson, O. R., Segal, G., and Shuman, H. A. (2004) *Science* **303,** 1358–1361
28. Kagan, J. C., Stein, M. P., Pypaert, M., and Roy, C. R. (2004) *J. Exp. Med.* **199,** 1201–1211
29. Dorer, M. S., Kirton, D., Bader, J. S., and Isberg, R. R. (2006) *PLoS Pathog.* **2,** e34
30. Urwyler, S., Nyfeler, Y., Lee, H., Mueller, L. N., Aebersold, R., and Hilbi, H. (2009) *Traffic* **10,** 76–87
31. Luo, Z. Q., and Isberg, R. R. (2004) *Proc. Natl. Acad. Sci. U. S. A.* **101,** 841–846
32. Weber, S. S., Ragaz, C., Reus, K., Nyfeler, Y., and Hilbi, H. (2006) *PLoS Pathog.* **2,** e46
33. Ragaz, C., Pietsch, H., Urwyler, S., Tiaden, A., Weber, S. S., and Hilbi, H. (2008) *Cell. Microbiol.* **10,** 2416–2433
34. De Matteis, M. A., and Godi, A. (2004) *Nat. Cell Biol.* **6,** 487–492
35. Di Paolo, G., and De Camilli, P. (2006) *Nature* **443,** 651–657
36. Godi, A., Pertile, P., Meyers, R., Marra, P., Di Tullio, G., Iurisci, C., Luini, A., Corda, D., and De Matteis, M. A. (1999) *Nat. Cell Biol.* **1,** 280–287
37. Blumental-Perry, A., Haney, C. J., Weixel, K. M., Watkins, S. C., Weisz, O. A., and Aridor, M. (2006) *Dev. Cell* **11,** 671–682
38. Albers, U., Tiaden, A., Spirig, T., Al Alam, D., Goyert, S. M., Gangloff, S. C., and Hilbi, H. (2007) *Microbiology* **153,** 3817–3829
39. Wiater, L. A., Marra, A., and Shuman, H. A. (1994) *Plasmid* **32,** 280–294
40. Dowler, S., Currie, R. A., Campbell, D. G., Deak, M., Kular, G., Downes, C. P., and Alessi, D. R. (2000) *Biochem. J.* **351,** 19–31
41. Mampel, J., Spirig, T., Weber, S. S., Haagensen, J. A. J., Molin, S., and Hilbi, H. (2006) *Appl. Environ. Microbiol.* **72,** 2885–2895
42. Vistica, J., Dam, J., Balbo, A., Yikilmaz, E., Mariuzza, R. A., Rouault, T. A., and Schuck, P. (2004) *Anal. Biochem.* **326,** 234–256
43. Laue, T. M., Shah, B. D., Ridgeway, T. M., and Pelletier, S. L. (1992) in *Analytical Ultracentrifugation in Biochemistry and Polymer Science* (Harding, S. E., ed) pp. 90–125, Royal Society of Chemistry, Cambridge, UK
44. Johnson, W. C. (1999) *Proteins* **35,** 307–312
45. Lobley, A., Whitmore, L., and Wallace, B. A. (2002) *Bioinformatics* (*Oxf.*) **18,** 211–212
46. Whitmore, L., and Wallace, B. A. (2004) *Nucleic Acids Res.* **32,** D593–D594
47. Mezzasalma, T. M., Kranz, J. K., Chan, W., Struble, G. T., Schalk-Hihi, C., Deckman, I. C., Springer, B. A., and Todd, M. J. (2007) *J. Biomol. Screen.* **12,** 418–428
48. McGuffin, L. J., Bryson, K., and Jones, D. T. (2000) *Bioinformatics* (*Oxf.*) **16,** 404–405
49. Balla, A., and Balla, T. (2006) *Trends Cell Biol.* **16,** 351–361

50. Bardill, J. P., Miller, J. L., and Vogel, J. P. (2005) *Mol. Microbiol.* **56,** 90–103

51. Ninio, S., Zuckman-Cholon, D. M., Cambronne, E. D., and Roy, C. R. (2005) *Mol. Microbiol.* **55,** 912–926

52. Cambronne, E. D., and Roy, C. R. (2007) *PLoS Pathog.* **3,** e188

53. Newton, H. J., Sansom, F. M., Bennett-Wood, V., and Hartland, E. L. (2006) *Infect. Immun.* **74,** 1683–1691

54. Newton, H. J., Sansom, F. M., Dao, J., McAlister, A. D., Sloan, J., Cianciotto, N. P., and Hartland, E. L. (2007) *Infect. Immun.* **75,** 5575–5585

55. Weber, S. S., Ragaz, C., and Hilbi, H. (November 18, 2008) *Cell. Microbiol.* 10.1111/j.1462–5822.2008.01266.

56. Stahelin, R. V., Karathanassis, D., Murray, D., Williams, R. L., and Cho, W. (2007) *J. Biol. Chem.* **282,** 25737–25747

57. Demmel, L., Gravert, M., Ercan, E., Habermann, B., Muller-Reichert, T., Kukhtina, V., Haucke, V., Baust, T., Sohrmann, M., Kalaidzidis, Y., Klose, C., Beck, M., Peter, M., and Walch-Solimena, C. (2008) *Mol. Biol. Cell* **19,** 1991–2002

58. Lemmon, M. A. (2008) *Nat. Rev. Mol. Cell Biol.* **9,** 99–111

59. Nagai, H., Cambronne, E. D., Kagan, J. C., Amor, J. C., Kahn, R. A., and Roy, C. R. (2005) *Proc. Natl. Acad. Sci. U. S. A.* **102,** 826–831

60. Laguna, R. K., Creasey, E. A., Li, Z., Valtz, N., and Isberg, R. R. (2006) *Proc. Natl. Acad. Sci. U. S. A.* **103,** 18745–18750

61. Pfeffer, S. R., Dirac-Svejstrup, A. B., and Soldati, T. (1995) *J. Biol. Chem.* **270,** 17057–17059

62. Seidel, R. D., III, Amor, J. C., Kahn, R. A., and Prestegard, J. H. (2004) *Biochemistry* **43,** 15393–15403

63. Godi, A., Di Campli, A., Konstantakopoulos, A., Di Tullio, G., Alessi, D. R., Kular, G. S., Daniele, T., Marra, P., Lucocq, J. M., and De Matteis, M. A. (2004) *Nat. Cell Biol.* **6,** 393–404